CLASSIFICATION: Biological Sciences / Physical Sciences (Chemistry)

TITLE: Structure of human endo-α-1,2-mannosidase (MANEA), an antiviral host-glycosylation target

AUTHORS: Łukasz F. Sobala[1], Pearl Z Fernandes[2], Zalihe Hakki[2], Andrew J Thompson[1], Jonathon D Howe[3], Michelle Hill[3], Nicole Zitzmann[3], Scott Davies[4], Zania Stamataki[4], Terry D. Butters[3], Dominic S. Alonzi[3], Spencer J Williams[2,*], Gideon J Davies[1,*]

AFFILIATIONS: 1. Department of Chemistry, University of York, YO10 5DD, United Kingdom. 2. School of Chemistry and Bio21 Molecular Science and Biotechnology Institute, University of Melbourne, Parkville, Victoria 3010, Australia. 3. Oxford Glycobiology Institute, Department of Biochemistry, University of Oxford, South Parks Road Oxford OX1 3QU, United Kingdom. 4. Institute for Immunology and Immunotherapy, University of Birmingham, Edgbaston, Birmingham B15 2TT, United Kingdom.

CORRESPONDING AUTHOR:

sjwill@unimelb.edu.au, ORCID 0000-0001-6341-4364

gideon.davies@york.ac.uk ORCID 0000-0002-7343-776X

ABSTRACT: Mammalian protein N-linked glycosylation is critical for glycoprotein folding, quality control, trafficking, recognition and function. N-linked glycans are synthesized from $Glc_3Man_9GlcNAc_2$ precursors that are trimmed and modified in the endoplasmic reticulum (ER) and Golgi apparatus by glycoside hydrolases and glycosyltransferases. Endo-α-1,2-mannosidase (MANEA) is the sole *endo*-acting glycoside hydrolase involved in N-glycan trimming and unusually is located within the Golgi, where it allows ER escaped glycoproteins to bypass the classical N-glycosylation trimming pathway involving ER glucosidases I and II. There is considerable interest in the use of small molecules that disrupt N-linked glycosylation as therapeutic agents for diseases such as cancer and viral infection. Here we report the structure of the catalytic domain of human MANEA and complexes with substrate-derived inhibitors, which provide insight into dynamic loop movements that occur upon substrate binding. We reveal structural features of the human enzyme that explain its substrate preference and the mechanistic basis for catalysis. The structures inspired the development of new inhibitors that disrupted host protein N-glycan processing of viral glycans and reduced infectivity of bovine viral diarrhea and dengue viruses in cellular models. These results may contribute to efforts of developing broad-spectrum antiviral agents and bring about a more detailed view of the biology of mammalian glycosylation. (205 words)

KEYWORDS: Glycobiology, viral infection, glycosylation, carbohydrate-active enzyme, enzyme inhibitor, mannosidase, N-glycan, enzyme

SIGNIFICANCE STATEMENT: The glycosylation of proteins is a major protein modification that occurs extensively in eukaryotes. Glycosidases in the secretory pathway that trim N-linked glycans play a key role in protein quality control and in the specific modifications leading to mature glycoproteins. Inhibition of glucosidases in the secretory pathway is a proven therapeutic strategy, and one with great promise in the treatment of viral disease. The enzyme endo-α-1,2-mannosidase, MANEA, provides an alternative processing pathway to evade glucosidase inhibitors. We report the 3D structure of human MANEA and complexes with bespoke enzyme inhibitors that we show act as antivirals for bovine viral diarrhea and human dengue viruses. The structure of MANEA will support inhibitor optimization and the development of more potent antivirals. (119 words)

Introduction

Asparagine (N) linked glycosylation is a protein modification that is widespread in eukaryotes and is essential for protein quality control and trafficking (1). N-Linked glycans contribute to protein structure and stability, receptor targeting, development and immune responses (2). N-Linked glycosylation occurs in the secretory pathway and is initiated in the lumen of the endoplasmic reticulum (ER) through co-translational transfer of the triantennary $Glc_3Man_9GlcNAc_2$ glycan from a lipid linked precursor (Fig. 1; see also (2-5)). Formation of mature glycoproteins requires the removal of the glucose residues, typically through the action of α-glucosidases I and II, which are localized within the rough ER. However, in most cell lines and in human patients genetic disruption of α-glucosidase I or II, or inhibition of their activities do not prevent the formation of mature glycoproteins, because of the action of Golgi endo-α-1,2-mannosidase (MANEA (6)). The action of MANEA provides a glucosidase independent pathway for glycoprotein maturation termed the endomannosidase pathway (7).

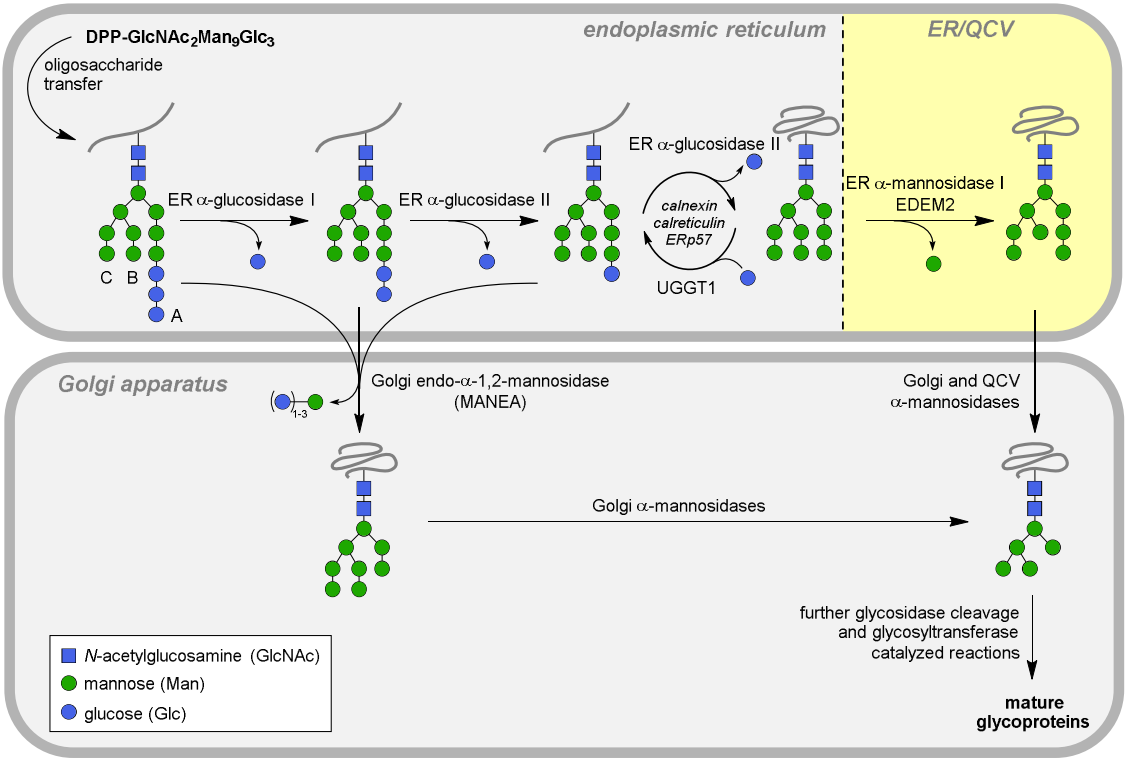

Figure 1. Simplified pathway for biosynthesis of N-linked glycans through the classical and endomannosidase pathways. *En bloc* transfer of the preformed $Glc_3Man_9GlcNAc_2$ tetradecasaccharide (branches labelled A/B/C) from the dolichol-precursor occurs co-translationally to Asn residues within the consensus sequence Asn-Xxx-Ser/Thr. Trimming of glucose residues can be achieved through the classical pathway involving sequential action of α-glucosidases I and II. Alternatively, Golgi endo-α-1,2-mannosidase (MANEA) provides a glucosidase independent pathway for glycoprotein maturation, through cleaving the glucose-

substituted mannose residues. ER mannosidase I resides in quality control vesicles (QCVs) (8). ER associated degradation of terminally misfolded glycoproteins is omitted.

MANEA is present chiefly in *cis*/*medial* Golgi (84%) and ER-Golgi intermediate compartment (ERGIC; 15%) (9) and allows trimming of glucosylated mannose residues from $Glc_{1\text{-}3}Man_9GlcNAc_2$ structures and B and C branch mannose-trimmed variants. MANEA action on $Glc_{1\text{-}3}Man_9GlcNAc_2$ results in cleavage of the glucosylated mannose in the A branch, releasing $Glc_{1\text{-}3}Man$ and $Man_8GlcNAc_2$; human MANEA acts faster on Glc_1Man than on $Glc_{2,3}Man$ glycans (10). The endomannosidase pathway allows processing of ER-escaped, glucosylated high-mannose glycans on glycoproteins that fold independently of the calnexin/calreticulin (CNX/CRT) folding cycle, allowing them to rejoin the downstream N-glycan maturation pathway. In murine BW6147 cells under normal conditions, flux through the endomannosidase pathway accounts for around 15% of total flux through the secretory pathway (11); under conditions of glucosidase blockade through knockout or inhibition, MANEA can support as much as 50% of normal glycoprotein flux, depending on cellular expression levels (11). MANEA activity accounts for the accumulation of Glc_3Man tetrasaccharide in the urine of a neonate suffering from CDG-IIb, a rare genetic disease caused by a deficiency of ER glucosidase I (MOGS) (12).

Most enveloped viruses (eg coronaviruses, retroviruses, ebolaviruses, hepatitis B virus (HBV), influenza viruses) contain glycoproteins within their envelope (13). Glycosylation is achieved by coopting host cell glycosylation machinery during replication. Substantial efforts have been deployed in the use of inhibitors of α-glucosidases I and II as antivirals (eg *N*-butyldeoxynojirimycin, 6-*O*-butanoylcastanospermine) for the treatment of HIV/AIDS (14), dengue (15, 16), and hepatitis B (17, 18) (reviewed in refs (19-21)). Inhibition of host glycosylation pathways, in particular ER glucosidases I and II and Golgi mannosidase I, interferes with the viral lifecycle by impairing protein folding and quality control, inducing the unfolded protein response, or mistrafficking of viral glycoproteins. These changes can lead to impairment of secretion (18, 22-24), fusion (25-27) or evasion of host immunity (28). Dwek and co-workers showed that when glucosidases are inhibited mature HBV viral glycoproteins are still produced, through the alternative processing provided by the endomannosidase pathway (29). However, the contribution of the endomannosidase pathway to viral protein assembly under normal conditions remains poorly studied, and the antiviral activity of inhibitors targeting MANEA has not been evaluated.

The *Homo sapiens* endo-α-1,2-mannosidase gene, *MANEA*, is located on chromosome 6. The *MANEA* gene has one isoform whose protein product, MANEA, is categorized as a member of the glycoside hydrolase (GH) family 99 in the Carbohydrate-Active enZyme (CAZy) database (30). *MANEA* encodes a protein 462 aa long that consists of a single pass, type II, membrane protein with a transmembrane helix followed by a stem region, followed by the catalytic domain (31). Here, we reveal the structure of the catalytic domain of human MANEA. Through complexes with substrate we reveal the architecture of the binding groove and identify key catalytic residues. We report structures with MANEA inhibitors that were designed based on the structure of the glucosylated high mannose N-glycan. Finally, we show that inhibitors of MANEA act as anti-viral agents against bovine viral diarrheal virus (BVDV) and dengue virus (DENV), confirming that MANEA is an anti-viral target.

Results

Expression and activity of Human MANEA GH99

In order to obtain soluble MANEA GH99 protein for structure-function studies to inform inhibitor design, attempts were made to express the gene. Initial failures with expression in CHO and HEK cells led us to consider bacterial gene expression. A truncated gene for MANEA, consisting of the catalytic domain beyond the stem domain, *i.e.* residues 98-462 (hereafter MANEA-Δ97), was synthesized in codon-optimized form. Expression trials in *E. coli* BL21(DE3) cells gave only insoluble protein, but we were inspired by a report (32) of soluble expression using cold-shock promotors (pCold-I vector) and co-expression of GroEL chaperones. Initial studies using lysogeny broth generated large quantities of insoluble GroEL and no soluble MANEA-Δ97 but by switching to Terrific Broth supplemented with glycerol and 20 mM $MgCl_2$ we obtained soluble MANEA-Δ97 in yields of approx. 2-3 mgL^{-1} (**Supplemental Figure 1A**, see Experimental procedures). The recombinant protein was purified using the encoded N-terminal His_6-tag, and was stable with a T_m of 50 □ (**Supplemental Figure 1B**).

Treatment of $GlcMan_9GlcNAc_2$ with recombinant MANEA-Δ97 released α-Glc-1,3-Man and $Man_8GlcNAc_2$ (**Supplemental Figure 1C**). Enzyme kinetics were measured using α-Glc-1,3-α-Man-1,2-α-Man-1,2-α-Man-OMe ($GlcMan_3OMe$) as substrate using a coupled assay in which the product α-1,2-Man-ManOMe is hydrolysed by α-mannosidase and the

resultant mannose quantified using a D-mannose/D-fructose/D-glucose detection kit (Megazyme, Inc.) (33). MANEA-Δ97 hydrolysed $GlcMan_3OMe$ with a k_{cat} of 27.7 ± 1.0 min^{-1} and K_M of 426 ± 33 μm (k_{cat}/K_M of 65 mM^{-1} min^{-1}) (**Supplemental Figure 1D**). The catalytic efficiency is similar to that displayed by a bacterial endo-α-1,2-mannanase from *Bacteroides thetaiotaomicron* on the epimeric Man_4OMe substrate (K_M = 2.6 mM, k_{cat} = 180 min^{-1}, k_{cat}/K_M = 69 mM^{-1} min^{-1}) (33). The E404Q variant of MANEA-Δ97 was inactive on this substrate, consistent with the proposed mechanism (34).

Development of MANEA inhibitors

Spiro, Spohr and coworkers reported the development of GlcDMJ as a cell-permeable inhibitor of MANEA (35, 36). The structure of GlcDMJ contains the well-known mannosidase iminosugar inhibitor deoxymannojirimycin (DMJ) modified with a glucosyl residue at the 3-position to enhance specificity and binding to MANEA by mimicking the substrate and benefitting from substrate-enzyme contacts in the -2 subsite. Thompson *et al.* reported the development of GlcIFG (37), which is also cell permeable (38), through a similar approach applied to the azasugar isofagomine (IFG). Subsequently, ManIFG was developed and shown to be a superior inhibitor of bacterial endo-α-1,2-mannanases (33). Fleet expressed concerns over the potential for α-glucosidase II catalyzed hydrolysis of GlcDMJ (39), potentially leading to a loss of inhibitor in cell-based systems, a problem that is also expected to apply to GlcIFG. Examination of the 3D X-ray structure of α-glucosidase II in complex with *N*-butyldeoxynojirimycin reveals binding of the sugar-shaped heterocycle involves a pocket-like active site that will not readily accommodate additional substituents (40). Conversely, it is known that MANEA can cleave $Glc_{1-3}Man$ substrates in which a substituent is tolerated at the 3-position of the glucosylated mannose. Therefore, we synthesized CyMe-GlcIFG, which bears a bulky cyclohexylmethyl substituent at the same position, in the expectation that it should be impervious to α-glucosidase II activity, yet still bind to MANEA.

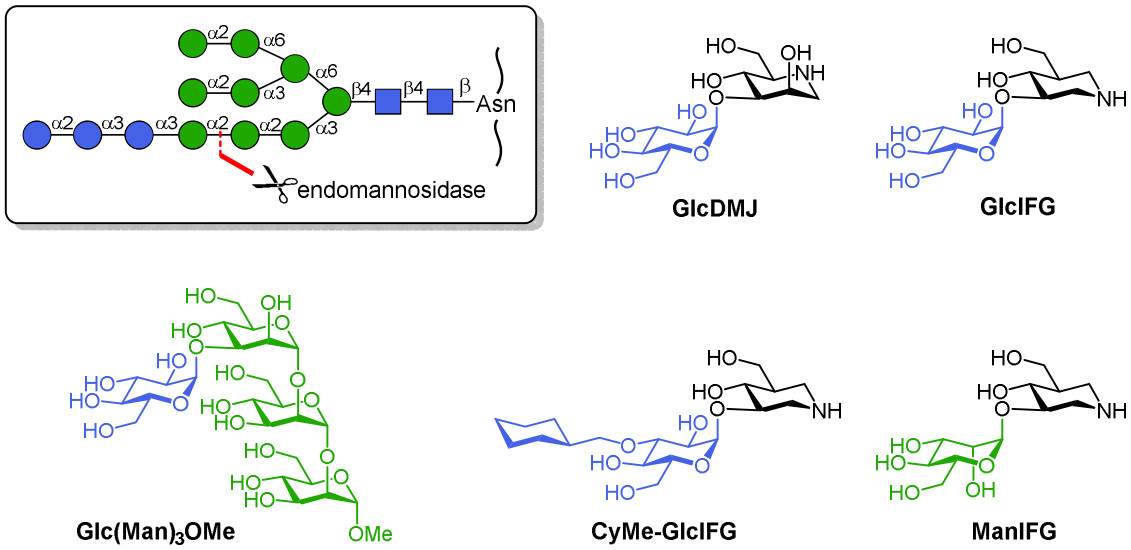

Figure 2. Substrates and inhibitors for MANEA inspired from the structure of the glucosylated N-glycan substrate. Inset: structure of $Glc_3Man_9GlcNAc_2$ showing the cleavage site of MANEA.

Isothermal titration calorimetry revealed that GlcIFG binds to MANEA-Δ97 with K_d = 19.6 ± 5.6 nM and ManIFG with K_d = 170 ± 32 nM. Whilst we were encouraged by preliminary studies on a bacterial MANEA homolog that showed that CyMeGlc-IFG bound better (K_d = 284 nM) than GlcIFG alone (K_d = 625 nM), on the human enzyme CyMe-GlcIFG bound less tightly that GlcIFG with K_d = 929 ± 52 nM (**Supplemental Figure 1E**), consistent with structural features observed subsequently (see below). Prioritizing scarce material for anti-viral work (*vide infra*) we did not measure K_d for GlcDMJ, which has previously been reported to have IC_{50} values of 1.7 to 5 μM (35, 39). MANEA thus exhibits a preference for inhibitors that match the stereochemistry of the substrate -2/-1 residues (GlcIFG versus ManIFG), which is the reverse of the preference of bacterial endo-α-1,2-mannanases for the same inhibitors (i.e. for *B. thetaiotaomicron* GH99: GlcIFG K_d = 625 nM; ManIFG K_d = 140 nM (33)).

Three-dimensional structure of human MANEA sheds light on eukaryotic enzyme specificity

Crystals of human MANEA-Δ97, **Figure 3A**, were obtained in several crystal forms (see Experimental). The initial crystal form, in space group $P2_12_12$, diffracted to around 2.25 Å resolution. Structure solution by molecular replacement (using the bacterial *Bx*GH99

(approx. 40% identity) as a search model) was successful leading to structures with R/R_{free} 18/22% (**Supplemental Table 1**). Unfortunately, this crystal form, whilst allowing description of the 3D fold, did not form ligand complexes due to occlusion of the active centre by the His_6-tag and a metal-ion assumed to be Ni^{2+}, with the integrity of the crystal lattice appearing to be mediated by this ion. A second crystal form, $P4_32_12$ gave data of lower resolution (3 Å) but in this case we were able to build a loop (131-141) absent in the first crystal form. Interestingly, the active centre was occupied by HEPES, a buffer that has been reported to inhibit rat endomannosidase (6); however, this crystal form could not be reliably reproduced.

An extensive screen of crystallization additives eventually yielded a crystal form amenable to ligand binding studies. Success was achieved with Anderson−Evans polyoxotungstate $[TeW_6O_{24}]^{6-}$ (TEW), which has been used on occasion in protein crystallography to act as a linking agent between molecules in the crystal lattice (examples include PDB 4OUA, 4PHI, 4Z13, 6G3S, 6QSE and 6N90; reviewed in Ref (41)). Using TEW and HEPES buffer, we obtained a new crystal form of MANEA-Δ97 in space group $P6_2$, which diffracted up to 1.8 Å resolution, generating largely anisotropic datasets. In this form, the proposed ligand binding site was again occupied by HEPES, with residues 191-201 poised to accept –2/–1 subsite ligands and +1/+2 subsites open. The co-crystallized HEPES buffer molecule could, in this case, be outcompeted by ligand soaking (the IC_{50} for HEPES shows weak binding, **Supplemental Figure S2**) and we obtained a series of complexes, including a binary complex of MANEA-Δ97 with GlcIFG, and a ternary complex with GlcIFG and α-1,2-mannobiose (structure and refinement statistics in **Supplemental Table 1**).

The overall 3D structure of human MANEA is a single domain $(\beta/\alpha)_8$ barrel with a (partially, see below) open active center in which Glu404 and Glu407 (human numbering, as part of a conserved **E**WH**E**) motif are the catalytic residues in a neighboring group participation mechanism that proceeds through an epoxide intermediate (34), **Figure 3B,C**. The structure is similar (Cα RMSD over 0.9 Å over 333 matched residues) to structures reported (37) for bacterial family GH99 endo-α-1,2-mannanases from *Bacteroides thetaiotaomicron* and *B. xylanisolvens*, with which MANEA shares 40% sequence identity. The positions of the –2 to +2 ligands in the bacterial and human GH99 proteins are equivalent and the sugar interactions in the –2 to +2 subsites (all of which bind mannosides

with identical linkages in both high-mannose N-glycans (MANEA) and yeast mannan (bacterial *endo*-α-1,2-mannanases (42)) are invariant.

A key difference between the substrates for the human and bacterial GH99 enzymes are the –2 sugar residues, which is glucose in high-mannose N-glycans, and mannose in yeast mannan. These differences are achieved by differences in recognition between the human and bacterial GH99 enzymes in the –2 subsite and its environs. Previously, it has been noted that in bacterial endo-α-1,2-mannanases Trp126 (in *B. xylanisolvens* GH99 (37)) forms a hydrophobic interaction with the C2 that was believed to be responsible for the selectivity of bacterial enzymes for ManMan versus GlcMan substrates. In MANEA, the equivalent residue is Tyr189, which makes a water-mediated interaction with O2 of Glc in the –2 subsite, **Figure 3 D,E**. Notably, we observed a loop (residues 191-201, hereafter the "–2 loop)", that was flexible and observed in different position in the different MANEA crystal forms (**Figure 3F**), but which was absent in the bacterial structures (**Supplemental Figure 3**). Two residues within the –2 loop are invariant across animal MANEAs: Asp195 and Gly198. Our structures reveal that Asp195 forms a hydrogen bond with the 3-OH of the –2 sugar (glucose) residue, and along with Asn197 H-bonding to O4, is a key determinant of binding of GlcMan structures. The second invariant residue, Gly198, enables the formation of a 195-198 turn thereby allowing residues 195, 196 and 197 to form hydrogen bonds with the –2 sugar (**Figure 3D,F)**.

Kukushkin *et al.* showed that MANEA isolated from human liver carcinoma cells processes triglucosylated N-glycans at a lower rate than monoglucosylated N-glycans (10). In the GlcIFG complex of MANEA, the –2 loop is closed over the active site, and in this conformation, triglucosylated N-glycans would be unable to bind to human MANEA. However, the other observed conformations show flexibility in the loop that could allow these extended structures to bind. Kukushkin *et al.* also noted that bovine MANEA did not process triglucosylated N-glycans. While both bovine and human MANEA possess the –2 loop, Kukushkin *et al.* identified a Ser227 (human) to Lys change in the bovine enzyme that they proposed contributed to the difference in specificity. Ser227 lies adjacent to, and points towards the –2 loop; the side chain of Lys226 (numbering as in bovine) may interact with the loop and reduce its mobility (**Figure 3F**). Interactions with the loop possibly explain why CyMe-GlcIFG binds nearly 50-fold more weakly than GlcIFG. Notably, bacterial GH99 endomannanases, which act on complex, extended yeast mannan substrates have open active sites and do not contain this loop. To test this hypothesis, we determined the structure of the

B. xylanisolvens GH99 with CyMe-GlcIFG (K_d 339 nM; tighter binding than GlcIFG alone, 625 nM) and indeed the loop occludes the cyclohexyl binding and it is visible (but mobile) in the density (**Supplemental Figure 4**)

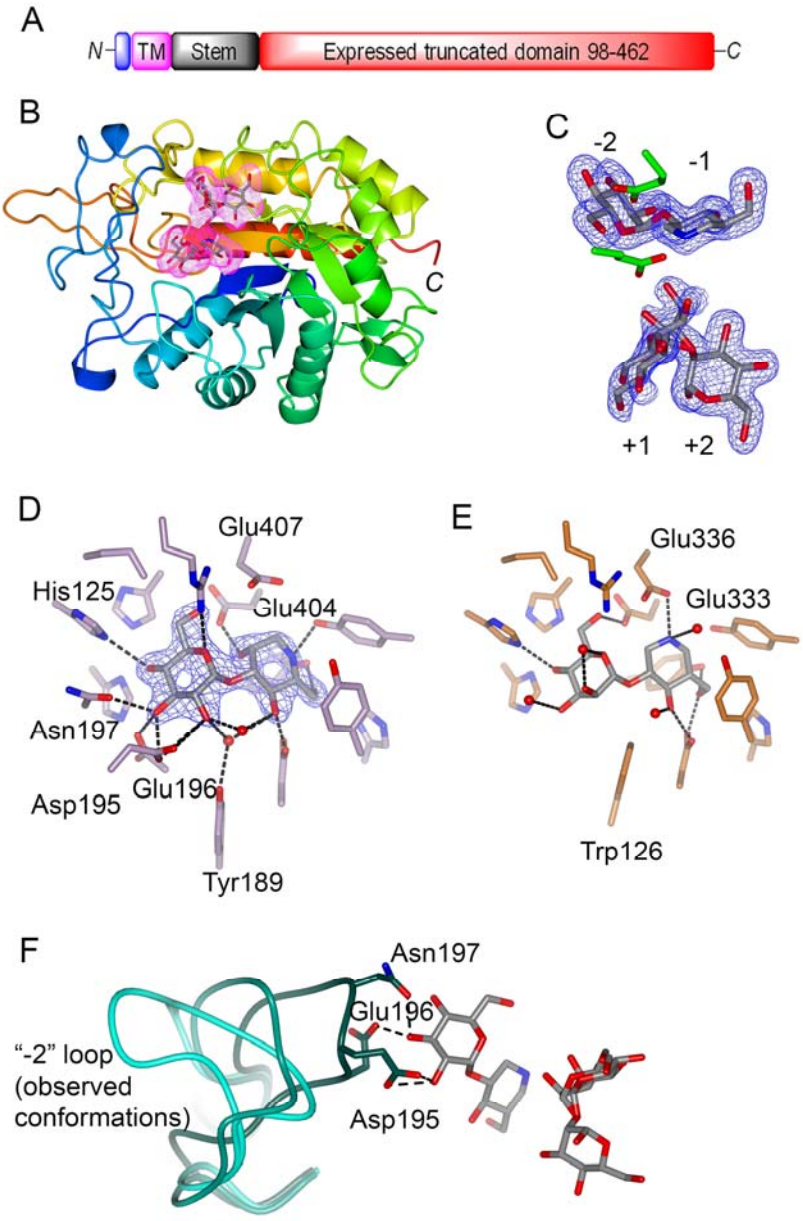

Figure 3: **3D X-ray structure of *Homo sapiens* MANEA endomannosidase and its complexes**. A. Domain structure of MANEA indicating the 98-462 domain that was expressed. B. 3D structure of MANEA, color ramped from N (blue) to C (red) terminus and with GlcIFG and α-1,2-mannobiose ligands shaded. C. Electron density for the ternary complex of MANEA with GlcIFG and α-1,2-mannobiose. 2m*Fo*-D*Fc* synthesis contoured at 0.4 $e^{-}/Å^3$. D. The –2 and –1 subsites of MANEA in complex with GlcDMJ, showing the

interactions and with key residues labeled. 2m*Fo*-D*Fc* synthesis contoured at 0.6 $e^{-}/Å^{3}$. E. The comparable –2 and –1 subsites of the bacterial endomannanase *Bx*GH99 involved in yeast mannan degradation, in complex with ManIFG (PDB 4V27). F. Residues 189-203 containing the flexible loop as observed in: MANEA-E333Q structure (cyan), MANEA+Ni^{2+} structure (darker cyan) and MANEA with GlcIFG and α–1,2 mannobiose structure (darkest cyan; ligand: grey). Hydrogen bonds with the –2 sugar are shown as dashed lines.

Human MANEA as a host cell antiviral target

To explore the potential of the endomannosidase pathway as an antiviral target, we studied the effect of MANEA inhibitors on replication of BVDV, a pestivirus of the *Flaviviridae* family. Reinfection assays showed that increasing concentrations of GlcIFG, the tightest binding ligand of MANEA, resulted in a decrease in the number of infected cells (measured as focus-forming units (FFU)) **Figure 4A**. Spiro and co-workers identified changes in the N-glycan structure of vesicular stomatitis virus G protein induced by the MANEA inhibitor GlcDMJ by demonstrating a change in susceptibility to hydrolysis by endo-β-*N*-acetylglucosaminidase (endo H) (43). Therefore, we digested BVDV envelope glycoproteins E1/E2 with endo H. Increased sensitivity of E1/E2 proteins to endo H cleavage was observed both in the case of GlcIFG and the glucosidase I/II inhibitor NAP-DNJ, indicating an increased prevalence of high mannose N-glycans. The increased sensitivity for GlcIFG was greater than for NAP-DNJ, most likely reflecting the higher concentration of the former. Treatment with a combination of GlcIFG and NAP-DNJ gave an even higher sensitivity to endo H treatment, consistent with more effective cessation of N-glycan processing by blocking the glucosidase and endomannosidase pathways. We next examined BVDV replication in the presence of a combination of GlcIFG and NAP-DNJ (**Figure 4C**). These data showed that the combination of GlcIFG and NAP-DNJ gave a greater reduction than either agent alone suggesting an additive antiviral effect from inhibiting both the α-glucosidase I/II and endomannosidase pathways. The addition of NAP-DNJ not only inhibits calnexin mediated folding and quality control but requires viral glycans to undergo processing by MANEA, hence potentiating the antiviral effect.

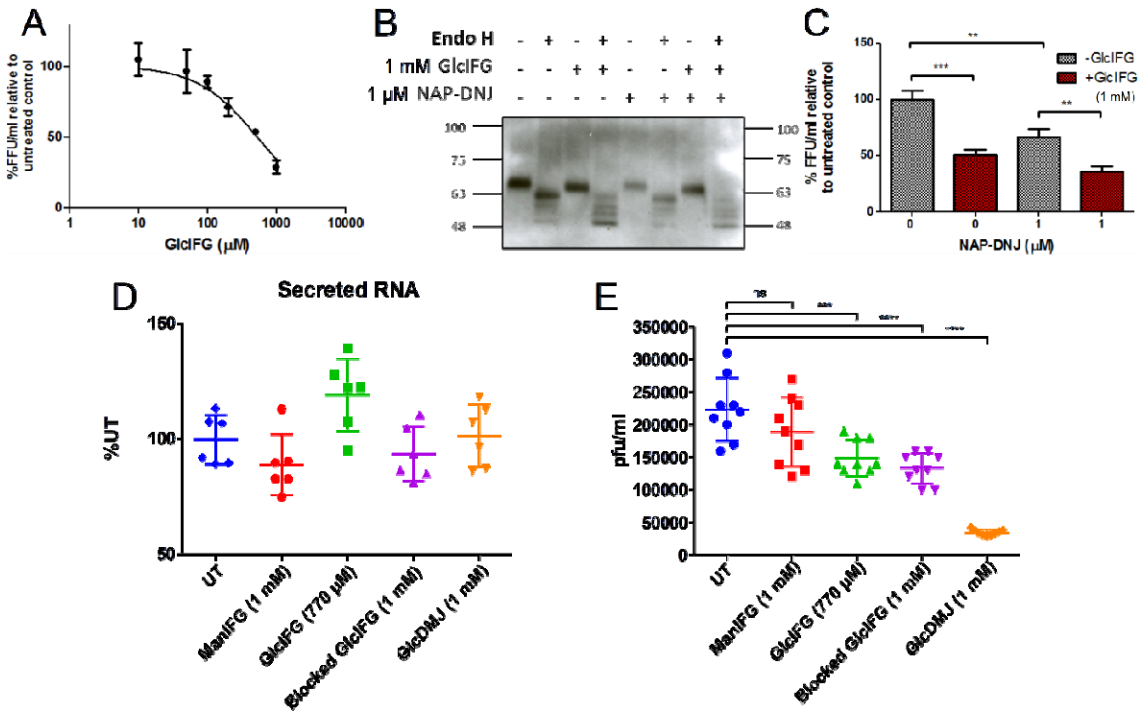

Figure 4. Anti-viral action of MANEA inhibitors. Results of (A,B,C) BVDV reinfection assays in MDBK cells and (D,E) DENV reinfection assays in Huh7.5 cells. (A) Percentage of FFU/ml relative to untreated cells at different concentrations of GlcIFG, at a multiplicity of infection of 1. (B) Effect of MANEA inhibition (GlcIFG) and ER glucosidase II inhibition (NAP-DNJ) on the susceptibility of glycans on the BVDV E1/E2 protein to cleavage by endoH. (C) The combined effects of NAP-DNJ and GlcIFG on BVDV infectivity, as measured by FFU/ml. Experiments performed in triplicate. (D) Secreted RNA levels in DENV infected Huh7.5 cells. (E) Reinfectivity plaque assay from DENV infected Huh7.5 cells. The horizontal bar in D and E indicates the mean.

To further define the antiviral potential of MANEA inhibitors, we extended these studies to DENV. The MANEA inhibitors GlcIFG, GlcDMJ, CyMe-GlcIFG and ManIFG were used to study levels of viral particle formation and infectivity. Viral particle formation, as assessed by secreted viral RNA, was unaffected by treatment with MANEA inhibitors (Figure 4D). However, treatment with GlcIFG, CyMe-GlcIFG and GlcDMJ caused a reduction in plaque number, showing that differences in glycosylation resulting from MANEA inhibition impair DENV infectivity. The greatest effect was seen for GlcDMJ, which reduced the number of plaque forming units by 6-fold. ManIFG, had no effect consistent with the weakest binding to MANEA. The antiviral effect observed is at a relatively high concentration but iminosugars are known to have difficulty in gaining access

to the secretory pathway (22). This proof of principle demonstrates GlcDMJ is a potential broad-spectrum antiviral with changes in glycosylation reducing infectivity of the progeny.

Summary

We report the 3D structure of Golgi endo-α-1,2-mannosidase, MANEA, a key eukaryotic N-glycosylation pathway glycosidase. This data provides a structural rationale to understand the change in specificity of this enzyme for mono-, di- and triglucosylated high mannose N-glycans. We also show the potential for MANEA inhibitors to alter N-glycan structures of viral envelope glycoproteins and reduce viral infectivity. MANEA processes $Glc_{1-3}Man_9GlcNAc_2$ structures and provides a pathway for glycoprotein maturation that is independent of the classical α-glucosidase I/II dependent pathways. Dwek and co-workers showed that miglustat (*N*-butyldeoxynojirimycin) treatment of HBV impaired viral DNA secretion and led to aberrant N-glycans on M glycoprotein, but that other viral glycoproteins displayed mature glycans that arose through the endomannosidase pathway (29). Conversely, Spiro showed that GlcDMJ treatment of VSV led to changes in G protein glycosylation (43). These prior studies and the present work demonstrate that different viral glycoproteins have varying degrees of dependence on the α-glucosidase I/II and endomannosidase pathways for maturation, and that inhibition of MANEA alone can alter infectivity of two encapsulated viruses. The human MANEA 3D structure, alongside demonstrated anti-viral activity of disaccharide imino and aza sugar inhibitors, provides a foundation for future inhibitor and drug development work. Given the devastating consequences of global outbreaks of viral disease, the present work highlights the potential for MANEA as a new target for host-directed antiviral agents exploiting viral glycoprotein biosynthesis.

ACKNOWLEDGEMENTS:

We thank the European Research Council (ERC-2012-AdG-32294 “Glycopoise”), the Australian Research Council (DP120101396, FT130100103, DP180101957) and the Royal Society for the Ken Murray Research Professorship to GJD. We thank Diamond Light Source UK for access to beamlines I03, I04 and I24 (proposals mx1221, mx12587 and mx18598). We acknowledge Jon Agirre for the help with generating a dictionary file for TEW and Eleanor Dodson for assistance with processing of the highly anisotropic datasets.

METHODS

Full methods are provided as Supplemental Information.

Expression, characterization and structure solution

Briefly, recombinant MANEA-Δ97 featuring an N-terminal His tag was expressed in *E. coli* from a pColdI system co-expressing the *groEL* and *groES* genes encoding the GroEL/ES chaperone system. Recombinant MANEA-Δ97 was purified by metal-ion affinity and cation-exchange chromatography. Extensive crystal screening identified five different crystal forms, with a condition including 1 m TEW (tellurium-centered Anderson–Evans polyoxotungstate $[TeW_6O_{24}]^{6-}$) allowing ligand binding studies without an occluded active site. Structure solution by molecular replacement, and refinement featured programs from the CCP4 suite (44). Structures, and observed data, have been deposited on the Protein Data Bank. MANEA activity was determined by mass spectrometry using $GlcMan_9GlcNAc_2$ as substrate with subsequent permethylation and analysis by MALDI-MS. Michael-Menten kinetics was performed using a coupled assay with $GlcMan_3OMe$ as substrate (33). Ligand binding thermodynamics were determined by isothermal titration calorimetry.

Viral Infectivity Studies

MDBK cells were infected with BVDV at a multiplicity of infection (MOI) of 1, followed by incubation with different concentrations of GlcIFG (0-1 mM) and in combination with NAP-DNJ for 24 h. Cell culture medium was harvested and serial dilutions were made and used to infect naive MDBK cells. Cells were incubated for 24 h, then washed and fixed with 4% (v/v) paraformaldehyde in PBS for 30 min. Following washing and blocking, cells were permeabilised and incubated with MAb103/105 (1:500 dilution in 5% milk-PBS; Animal Health Veterinary Laboratories Agency, Weybridge, UK) for 1 h. Incubation with anti-mouse FITC-conjugated secondary antibody (1:500 dilution in 5% milk-PBS; Sigma) and staining with 4′,6-diamidino-2-phenylindole allowed counting of fluorescent foci and calculation of virus titers (fluorescent focus units (FFU)/ml). The samples obtained after treatment for 24 h were treated with Endo H and separated by SDS–PAGE under non-reducing conditions. The membrane produced following transfer was probed with MAb214 primary antibody and then visualized with anti-mouse horseradish peroxidase secondary antibody (1:1000; Dako) for 1 h.

Huh7.5 cells were infected for 2 h with 50 µL of DENV2 strain 16681 at an MOI of 0.1. The inoculum was removed and replaced with 200 µL of growth media with drug at concentrations as indicated in triplicate, and the infected cells were incubated with drug for 2 d. The supernatant was harvested. DENV RNA in cell culture supernatants was isolated according to the manufacturer's protocol for Direct-zol RNA MiniPrep Kit (Zymo Research) and assayed by qRT-PCR. Samples were read in technical duplicate and compared to a standard curve generated from high-titer viral RNA isolated from C6/36-grown DENV2. 95% confidence intervals were determined based on biological and technical variation and graphed using Prism 6 (GraphPad Software, Inc). The infectious DENV titres in supernatants collected were evaluated by plaque assay.

REFERENCES:

1. Molinari M (2007) N-glycan structure dictates extension of protein folding or onset of disposal. *Nature chemical biology* 3(6):313-320.
2. Varki A (2017) Biological roles of glycans. *Glycobiology* 27(1):3-49.
3. Ohtsubo K & Marth JD (2006) Glycosylation in Cellular Mechanisms of Health and Disease. *Cell* 126(5):855-867.
4. Lombard J (2016) The multiple evolutionary origins of the eukaryotic N-glycosylation pathway. *Biology Direct* 11(1):36.
5. Aebi M (2013) N-linked protein glycosylation in the ER. *Biochimica et Biophysica Acta (BBA) - Molecular Cell Research* 1833(11):2430-2437.
6. Lubas WA & Spiro RG (1988) Evaluation of the role of rat liver Golgi endo-alpha-D-mannosidase in processing N-linked oligosaccharides. *J Biol Chem* 263(8):3990-3998.
7. Lubas WA & Spiro RG (1987) Golgi endo-α-D-mannosidase from rat liver, a novel N-linked carbohydrate unit processing enzyme. *J. Biol. Chem.* 262(8):3775-3781.
8. Shenkman M & Lederkremer GZ (2019) Compartmentalization and Selective Tagging for Disposal of Misfolded Glycoproteins. *Trends Biochem Sci* 44(10):827-836.
9. Zuber C*, et al.* (2000) Golgi Apparatus Immunolocalization of Endomannosidase Suggests Post-Endoplasmic Reticulum Glucose Trimming: Implications for Quality Control. *Molecular Biology of the Cell* 11(12):4227-4240.
10. Kukushkin NV, Easthope IS, Alonzi DS, & Butters TD (2012) Restricted processing of glycans by endomannosidase in mammalian cells. *Glycobiology* 22(10):1282-1288.
11. Moore SE & Spiro RG (1990) Demonstration that Golgi endo-alpha-D-mannosidase provides a glucosidase-independent pathway for the formation of complex N-linked oligosaccharides of glycoproteins. *J Biol Chem* 265(22):13104-13112.
12. De Praeter CM*, et al.* (2000) A Novel Disorder Caused by Defective Biosynthesis of N-Linked Oligosaccharides Due to Glucosidase I Deficiency. *The American Journal of Human Genetics* 66(6):1744-1756.
13. Bagdonaite I & Wandall HH (2018) Global aspects of viral glycosylation. *Glycobiology* 28(7):443-467.
14. Fischl MA*, et al.* (1994) The safety and efficacy of combination N-butyl-deoxynojirimycin (SC-48334) and zidovudine in patients with HIV-1 infection and 200-500 CD4 cells/mm3. *J Acquir Immune Defic Syndr (1988)* 7(2):139-147.
15. Sayce AC*, et al.* (2016) Iminosugars Inhibit Dengue Virus Production via Inhibition of ER Alpha-Glucosidases--Not Glycolipid Processing Enzymes. *PLoS Negl Trop Dis* 10(3):e0004524.
16. Warfield KL*, et al.* (2020) Targeting Endoplasmic Reticulum alpha-Glucosidase I with a Single-Dose Iminosugar Treatment Protects against Lethal Influenza and Dengue Virus Infections. *J Med Chem* 63(8):4205-4214.
17. Lu X*, et al.* (1997) Aberrant trafficking of hepatitis B virus glycoproteins in cells in which N-glycan processing is inhibited. *Proc Natl Acad Sci U S A* 94(6):2380-2385.
18. Lu X, Mehta A, Dwek R, Butters T, & Block T (1995) Evidence That N-Linked Glycosylation Is Necessary for Hepatitis B Virus Secretion. *Virology* 213(2):660-665.
19. Dwek RA, Butters TD, Platt FM, & Zitzmann N (2002) Targeting glycosylation as a therapeutic approach. *Nat. Rev. Drug Discov.* 1(1):65-75.
20. Chang J, Block TM, & Guo JT (2013) Antiviral therapies targeting host ER alpha-glucosidases: current status and future directions. *Antiviral Res* 99(3):251-260.
21. Williams SJ & Goddard-Borger ED (2020) A case for repurposing α-glucosidase inhibitors for the treatment of COVID-19. *Biochemical Society Transactions* in press.
22. Alonzi DS, Scott KA, Dwek RA, & Zitzmann N (2017) Iminosugar antivirals: the therapeutic sweet spot. *Biochemical Society Transactions* 45(2):571-582.
23. Block TM*, et al.* (1994) Secretion of human hepatitis B virus is inhibited by the imino sugar N-butyldeoxynojirimycin. *Proc Natl Acad Sci U S A* 91(6):2235-2239.

24. Mehta A, Lu X, Block TM, Blumberg BS, & Dwek RA (1997) Hepatitis B virus (HBV) envelope glycoproteins vary drastically in their sensitivity to glycan processing: Evidence that alteration of a single N-linked glycosylation site can regulate HBV□secretion. *PNAS* 94(5):1822-1827.
25. Dedera D, Vander Heyden N, & Ratner L (1990) Attenuation of HIV-1 Infectivity by an Inhibitor of Oligosaccharide Processing. *AIDS Research and Human Retroviruses* 6(6):785-794.
26. Dedera DA, Gu R, & Ratner L (1992) Role of asparagine-linked glycosylation in human immunodeficiency virus type 1 transmembrane envelope function. *Virology* 187(1):377-382.
27. Ratner L, Vander Heyden N, & Dedera D (1991) Inhibition of HIV and SIV infectivity by blockade of α-glucosidase activity. *Virology* 181(1):180-192.
28. Francica JR*, et al.* (2010) Steric Shielding of Surface Epitopes and Impaired Immune Recognition Induced by the Ebola Virus Glycoprotein. *PLOS Pathogens* 6(9):e1001098.
29. Mehta A, Lu X, Block TM, Blumberg BS, & Dwek RA (1997) Hepatitis B virus (HBV) envelope glycoproteins vary drastically in their sensitivity to glycan processing: evidence that alteration of a single N-linked glycosylation site can regulate HBV secretion. *Proc. Natl. Acad. Sci. USA* 94(5):1822-1827.
30. Lombard V, Golaconda Ramulu H, Drula E, Coutinho PM, & Henrissat B (2014) The carbohydrate-active enzymes database (CAZy) in 2013. *Nucleic Acids Research* 42(D1):D490-D495.
31. Hamilton SR*, et al.* (2005) Intact {alpha}-1,2-endomannosidase is a typical type II membrane protein. *Glycobiology* 15(6):615-624.
32. Dedola S*, et al.* (2016) Direct assay for endo-α-mannosidase substrate preference on correctly folded and misfolded model glycoproteins. *Carbohydrate Research* 434:94-98.
33. Hakki Z*, et al.* (2015) Structural and kinetic dissection of the *endo*-α-1,2-mannanase activity of bacterial GH99 glycoside hydrolases from *Bacteroides* spp. *Chem. Eur. J.* 21(5):1966-1977.
34. Sobala LF*, et al.* (2020) An Epoxide Intermediate in Glycosidase Catalysi. *ACS Central Science* in press.
35. Hiraizumi S, Spohr U, & Spiro RG (1993) Characterization of endomannosidase inhibitors and evaluation of their effect on N-linked oligosaccharide processing during glycoprotein biosynthesis. *J Biol Chem* 268(13):9927-9935.
36. Spohr U, Bach M, & Spiro R (1993) Inhibitors of endo-alpha-mannosidase .2. 1-deoxy-3-0-(alpha-D-glucopyranosyl)-mannojirimycin and congeners modified in the mannojirimycin unit. . *Can J Chem* 71:1928-1942.
37. Thompson AJ*, et al.* (2012) Structural and mechanistic insight into N-glycan processing by endo-α-mannosidase. *PNAS* 109(3):781-786.
38. Alonzi DS*, et al.* (2013) Glycoprotein misfolding in the endoplasmic reticulum: identification of released oligosaccharides reveals a second ER-associated degradation pathway for Golgi-retrieved proteins. *Cell. Mol. Life Sci.* 70(15):2799-2814.
39. Ardron H*, et al.* (1993) Synthesis of 1,5-dideoxy-3-O-(α-D-mannopyranosyl)-1,5-imino-D-mannitol and 1,5-dideoxy-3-O-(α-D-glucopyranosyl)-1,5-imino-D-mannitol: Powerful inhibitors of endomannosidase. *Tetrahedron: Asymmetry* 4:2011-2024.
40. Caputo AT*, et al.* (2016) Structures of mammalian ER alpha-glucosidase II capture the binding modes of broad-spectrum iminosugar antivirals. *Proc Natl Acad Sci U S A* 113(32):E4630-4638.
41. Bijelic A & Rompel A (2017) Ten Good Reasons for the Use of the Tellurium-Centered Anderson-Evans Polyoxotungstate in Protein Crystallography. *Acc Chem Res* 50(6):1441-1448.
42. Cuskin F*, et al.* (2015) Human gut Bacteroidetes can utilize yeast mannan through a selfish mechanism. *Nature* 517(7533):165-169.

43. Karaivanova VK, Luan P, & Spiro RG (1998) Processing of viral envelope glycoprotein by the endomannosidase pathway: evaluation of host cell specificity. *Glycobiology* 8(7):725-730.

44. Potterton L*, et al.* (2018) CCP4i2: the new graphical user interface to the CCP4 program suite. *Acta Crystallographica Section D* 74(2):68-84.